Covalently Bound pH-Indicator Dyes at Selected Extracellular or Cytoplasmic Sites in Bacteriorhodopsin. 1. Proton Migration along the Surface of Bacteriorhodopsin Micelles and Its Delayed Transfer from Surface to Bulk†

Peter Scherrer,*,‡,|| Ulrike Alexiev,‡ Thomas Marti,§,# H. Gobind Khorana,§ and Maarten P. Heyn*,‡

Biophysics Group, Department of Physics, Freie Universität Berlin, Arnimallee 14, D-14195 Berlin, Germany, and Departments of Biology and Chemistry, Massachusetts Institute of Technology, Cambridge, Massachusetts 02139

Received May 6, 1994; Revised Manuscript Received August 25, 1994⊗

ABSTRACT: The kinetics of the light-induced release and uptake of protons was monitored with the optical pH-indicator fluorescein covalently bound to various sites on the extracellular and cytoplasmic surfaces of bacteriorhodopsin. Selective labeling was achieved by reacting (iodoacetamido)fluorescein with the single cysteine residues in bacteriorhodopsin introduced at the desired positions by site-directed mutagenesis. All measurements were performed with bacteriorhodopsin micelles in phospholipid/detergent mixtures in 150 mM KCl at 22 °C, pH 7.3. Neither the replacements by cysteine nor the subsequent labeling affected the absorption spectrum of bacteriorhodopsin and the rise times of the M intermediate. Only the decay of M was altered for some bacteriorhodopsin mutants with cysteine residues on the cytoplasmic side. The proton release time detected with fluorescein attached to the extracellular surface (the proton release side) at position 72 (in the loop connecting helices B and C) or 130 (DE loop) was 22 ± 4 μs, clearly faster than that measured with pyranine in the aqueous bulk phase (125 ± 10 μs for wild-type and all mutants studied). For bacteriorhodopsin mutants labeled at positions 35, 101, 160, 229, and 231 in the cytoplasmic loop region (the proton uptake side), the released proton was observed with a time of 61 ± 4 μs. This was about 3-fold slower than the release time on the extracellular side, but still significantly faster than that measured with pyranine in the bulk phase. These results suggest that the released protons are retained on the micellar surface and move more rapidly along this surface to the cytoplasmic side than from the surface to the bulk medium. This conclusion is supported by experiments in which the proton mobility along the micellar surface was varied by adding phospholipids with headgroups of different pK_a's to the bacteriorhodopsin/CHAPS micelles. With the label on the cytoplasmic side, the amplitude of the light-induced transient protonation change increased or decreased, respectively, when DMPC (pK 2.2; proton dwell time ≈ 10 ns) or DMPA (pK 8.0; proton dwell time ≈ 10 ms) was added. However, no effect of the phospholipids was detected with the indicator on the extracellular side. These observations of faster proton diffusion along the micellar surface than their equilibration from the surface to the bulk support bioenergetic models of efficient proton coupling along the membrane surface between proton sources and sinks. Our data also demonstrate that a probe bound to the extracellular (proton release) surface is required to detect the actual appearance of the pumped proton on the protein surface and to correlate it with a specific photocycle intermediate.

Bacteriorhodopsin (bR)[1] is a seven helical transmembrane protein in the purple membrane of *Halobacterium salinarium* and functions as a light-driven proton pump [for a review, see Stoeckenius and Bogomolni (1982), Lanyi (1992), Oesterhelt et al. (1992), and Rothschild (1992)]. Like visual pigments, bR contains a retinylidene chromophore (Oesterhelt & Stoeckenius, 1971) with a protonated retinal Schiff base linkage to Lys-216 (Lewis et al., 1974). When illuminated, the chromophore undergoes a cyclic photoreaction comprising at least five spectroscopically distinct intermediates (Lozier et al., 1975). In the transition between the L and M intermediates, the Schiff base deprotonates, and a proton is released on the extracellular side of the membrane on roughly the same time scale. During the decay of M,

† This work was supported by grants from the Deutsche Forschungsgemeinschaft (Sfb 312-B1) and from the BMFT (03-HE3FUB) to M.P.H. and by a grant (GM 28289) from the National Institutes of Health to H.G.K.

* Correspondence could be addressed to either author.

‡ Freie Universität Berlin.

§ Massachusetts Institute of Technology.

|| Present address: Liposome Research Group, Department of Biochemistry, University of British Columbia, 2146 Health Sciences Mall, Vancouver, BC V6T 1Z3, Canada.

Present address: Bernhard Nocht Institute for Tropical Medicine, D-20359 Hamburg, Germany.

⊗ Abstract published in *Advance ACS Abstracts,* October 15, 1994.

[1] Abbreviations: bR, bacteriorhodopsin; bO, bacterioopsin; ebR, wild-type bR expressed in *Escherichia coli*; DMPC, 1,2-dimyristoyl-*sn*-glycero-3-phosphatidylcholine; CHAPS, 3-[(3-cholamidopropyl)-dimethylammonio]-1-propanesulfonate; MOPS, 4-morpholinepropanesulfonate; Tris, tris(hydroxymethyl)aminomethane; DMPA, 1,2-dimyristoyl-*sn*-glycerol-3-phosphatidic acid; DMF, dimethylformamide; EDTA, ethylenediaminetetraacetic acid; DTT, 1,4-dithio-DL-threitol; SDS, sodium dodecyl sulfate; IAF, 5-(iodoacetamido)fluorescein; CAF, fluorescein bound to cysteine (cysteine−(thioacetamido)fluorescein); AF, fluorescein bound to cysteine in bacteriorhodopsin; pK_{app}, apparent pK, the pK determined at the given ionic strength; τ_D, dwell time. The mutant bRs are characterized by the replaced amino acids as follows: the letter before the number indicates the original amino acid in that position while the letter following the number represents the substituting amino acid using single letter code (e.g., V130C: valine in position 130 is replaced by cysteine).

0006-2960/94/0433-13684$04.50/0

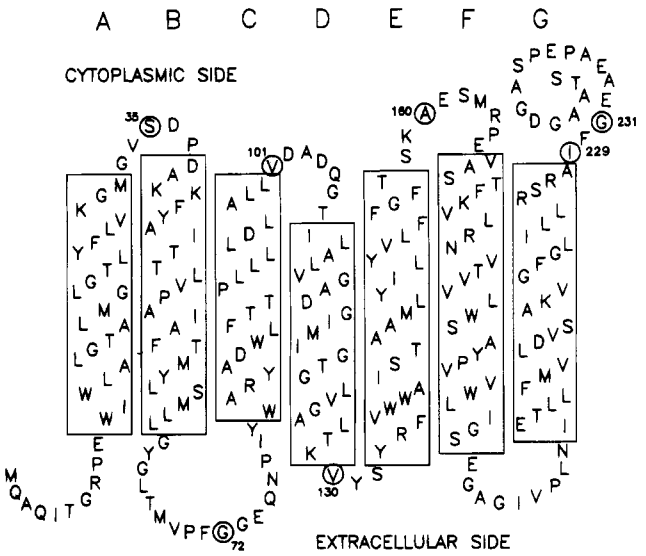

FIGURE 1: Secondary structural model of bacteriorhodopsin. The residues changed to cysteine are circled.

the Schiff base is reprotonated, and this is accompanied by proton uptake from the cytoplasmic side of the membrane. Flash−induced release and uptake of protons in purple membrane suspensions have been detected with pH−indicator dyes like 7-hydroxycoumarin (Lozier et al., 1976; Scherrer et al., 1981), pyranine (Drachev et al., 1984; Grzesiek & Dencher, 1986), or phenol red (Varo & Lanyi, 1990) which were added to the bulk medium. The proton release kinetics as measured with these indicators was considerably slower than the kinetics of the formation of the M intermediate. The proton release kinetics was accelerated in the presence of small buffer concentrations (Drachev et al., 1984; Grzesiek & Dencher, 1986). For a better understanding of the mechanism of the proton pump, it is important to establish if a close coupling exists between the kinetics of the proton release and the formation of the M intermediate. To detect the actual appearance of the proton on the surface of the protein, Heberle and Dencher (1990, 1992) linked the indicator fluorescein to the ϵ-amino group of lysine(s) on the purple membrane surface and observed a clearly faster proton release compared to the indicators in the aqueous phase.

The goal of the present work was to develop a general method for the attachment of a pH-indicator dye to any given position on the extracellular or cytoplasmic side of bacteriorhodopsin and to monitor the light-induced proton release and uptake at these sites. Site-directed mutagenesis has enabled the introduction of a cysteine residue at any given position in bacteriorhodopsin, and the reactive sulfhydryl group of cysteine can be used to attach probes to measure proton release and uptake. This method is facilitated by the absence of cysteine in native bR. In the present work, we bound fluorescein to the cysteine residues in the positions shown in Figure 1 using the iodoacetamido derivative. Fluorescein has a strongly pH-dependent absorption at 490 nm (Fothergill, 1964). To detect the proton concentration changes in the aqueous bulk phase, we used the negatively charged pH-indicator pyranine (Kano & Fendler, 1978). This method allowed us to monitor the light-induced proton release and uptake at any given position on the protein surface and in the aqueous bulk phase. The release times detected by this method on either side of bR were clearly faster than the one measured in the aqueous bulk phase. Further, we found significant and consistent differences in the proton release times as recorded by probes on the extracellular and cytoplasmic surface of bR. The data indicate that the protons released on the extracellular surface are retained at the surface and diffuse more rapidly along the micellar surface to the cytoplasmic side than into the bulk phase. These findings support the concept of localized coupling between proton sources (e.g., bR) and sinks (e.g., H^+ −ATP−synthase) by lateral proton flow along the surface and were already briefly described in an earlier paper (Scherrer et al., 1992). In addition, our results show conclusively that for proper time resolution of proton release a surface-bound dye on the extracellular side is required.

In the accompanying paper (Alexiev et al., 1994b), the improved time resolution for the detection of the proton is used to investigate the possible kinetic coupling between the rise of M and the release of protons and to search for differences in the local proton release time.

MATERIALS AND METHODS

Chemicals. 3-[(3-Cholamidopropyl)dimethylammonio]-1-propanesulfonate (CHAPS); 1,2-dimyristoyl-*sn*-glycero-3-phosphatidylcholine (DMPC); 1,4-dithio-DL-threitol (DTT); dimethylformamide (DMF); 4-morpholinepropanesulfonate (MOPS); and tris(hydroxymethyl)aminomethane (Tris) were obtained from Sigma. 1,2-Dimyristoyl-*sn*-glycero-3-phosphatidic acid (DMPA) was from Calbiochem. Ethylenediaminetetraacetic acid (EDTA), glutathione (reduced), and sodium dodecyl sulfate (SDS) were from Fluka. Sephadex G-25 (fine) was from Pharmacia, and 5-(iodoacetamido)-fluorescein (IAF) was from Molecular Probes.

Bacterioopsin Mutants. Methods for the construction of mutant opsin genes containing amino acid replacements by cysteine, their expression in *Escherichia coli*, and the purification of the apoproteins have been described (Flitsch & Khorana, 1989; Marti et al., 1991).

Renaturation of bO Mutant Proteins and Chromophore Formation. The previously described renaturation procedure (Liao et al., 1983) was modified as follows: The purified bO mutant proteins were stored in freeze-dried state. They contained approximately 5 mg of protein ($\approx$0.2 μmol) and 25 mg of SDS. The solid was dissolved in 1 mL of 100 mM NaCl containing 2 mM DTT, and the solution was incubated under argon for 30 min at room temperature. A 1-mL solution of 2% CHAPS, 2% DMPS, and 20 mM $NaPO_4$ buffer at pH 6.2 was added, followed by 25 μL (0.25 μmol) of an ethanolic solution (10 mM) of *all-trans*-retinal and 100 μL of 4 M KCl. Excess lipids, detergents, and buffer were removed by chromatography on a 12−15-mL Sephadex G-25 column preequilibrated and eluted with 0.1% CHAPS, 0.0025% DMPC, and 150 mM KCl.

Derivatization of Cysteine Containing bR by Reaction with (Iodoacetamido)fluorescein (IAF). A stock solution of 20 mM 5-IAF was prepared by first dissolving IAF in DMF, not exceeding 15% (v/v) of final volume, and then adding 100 mM Tris buffer, pH 8.0, to give the desired concentration. The cysteine mutant bR (0.1 μmol) in 1 mL of a solution containing 0.1% CHAPS, 0.0025% DMPC, 150 mM KCl, 4 μM EDTA, 0.1 mM DTT, and 50 mM Tris buffer (pH 8.0) was reacted with 50 μL of 20 mM 5-IAF (1 μmol) for 30 min at room temperature under argon. The reaction

was stopped by the addition of 100 μL of 200 mM glutathione (20 μmol) and 20 mM DTT (2 μmol). The excess reagents were removed by chromatography on a 12-mL Sephadex G-25 column equilibrated with 0.1% CHAPS, 0.0025% DMPC, and 150 mM KCl. For the separation of the noncovalently bound fluorescein, a larger than theoretical column size was required since fluorescein has a considerable affinity for the micelles. The best separation was obtained when the G-25 gel was pretreated with 1 mL of 2% DMPC and 2% CHAPS, followed by preequilibration with 0.1% CHAPS, 0.0025% DMPC, and 150 mM KCl. Some DMPC bound to the resin and showed a high affinity for fluorescein, retarding it greatly.

The stoichiometry of fluorescein incorporation per bR molecule was determined spectroscopically using a molar extinction coefficient of $\epsilon = 68\,000\ M^{-1}\ cm^{-1}$ (Molecular Probes) for the alkaline form of fluorescein at 495 nm and of $\epsilon = 52\,000\ M^{-1}\ cm^{-1}$ for bR at 550 nm (London & Khorana, 1982).

Flash spectroscopy was performed as described elsewhere (Otto et al., 1989). The excitation was with 10-ns pulses of 3−6 mJ of energy at 590 nm.

Flash-induced proton release and uptake were detected in the aqueous bulk medium of the micellar suspension containing 4−10 μM bR in 0.1% CHAPS, 0.0025% DMPC, and 150 mM KCl by measuring the difference of the flash-induced absorbance change at 450 nm between samples with and without 45 μM pyranine at pH 7.3 and 22 °C (DIFPY). The light-induced proton concentration change with fluorescein on the bR surface was measured by the flash-induced absorbance difference at 495 nm between samples with and without 10 mM MOPS buffer at pH 7.3 and 22 °C (DIFAF).

RESULTS

Characterization of ebR−Micelle System for Flash Photolysis Experiments. The functional activity of membrane proteins in mixed protein/lipid/detergent micelles is usually dependent on the nature of detergents and lipids present and on their relative concentrations. For bR, the kinetics of the photocycle intermediates are influenced by the detergent used in micelles (Milder et al., 1991). To obtain optimal renaturation (typically 80−90%) of the SDS containing bO samples, an excess of DMPC and CHAPS was necessary. After the renaturation, the SDS could be removed together with the excess CHAPS/DMPC by chromatography on a Sephadex G-25 column, and the desired bR/DMPC/CHAPS ratios were obtained. We found a strong effect of the bR/lipid/detergent ratio on the photocycle kinetics. Therefore, we searched for conditions where the photocycle kinetics are unaffected by small variations in the bR/lipid/detergent ratios as a result of small changes in the bR concentration and where the protein−micelle system is stable for weeks.

Thus, the lipid (DMPC) and detergent (CHAPS) concentration ratios in the ebR/lipid/detergent micelles were varied, and the effects on the kinetics of the M intermediate were analyzed (Figure 2). An increase in the CHAPS and/or DMPC concentration resulted in a slower M decay. The same protein/lipid/detergent ratio with different final concentrations showed the same kinetics for the M-intermediate. In 0.1% CHAPS, 0.0025% DMPC, and 150 mM KCl, a change in the protein concentration between 4 and 10 μM bR (this corresponds to a bR/lipid/detergent ratio of 1/8/330 to 1/3/125) did not cause any change in the M kinetics. Moreover, the kinetics of the M-intermediate (Figure 2, trace a) was most similar to that of native bR. Figure 3b displays the contour plot of a complete photocycle of ebR, measured from 370 to 690 nm in steps of 20 nm. For comparison, a contour plot of the photocycle of purple membrane is presented in Figure 3a and shows that the same intermediates occur. The main difference is a faster rise of M in the

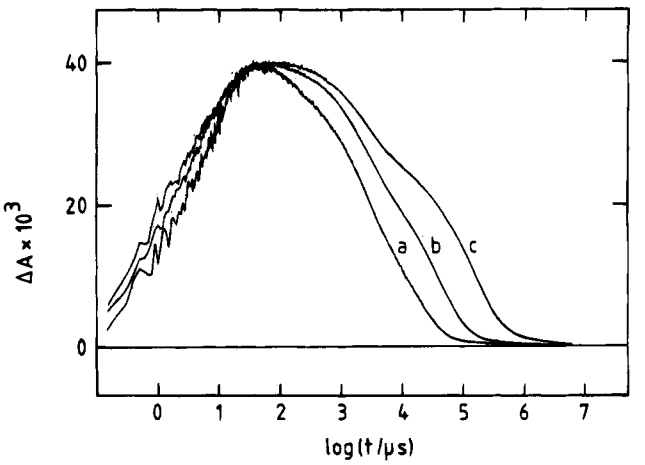

FIGURE 2: Dependency of the kinetics of the photocycle intermediate M_{412} of ebR on the CHAPS concentration. Time course of the flash-induced absorbance changes of bR at 410 nm and 22 °C, pH 7.3, in 150 mM KCl and (a) 0.1% CHAPS, 0.0025% DMPC, 4−10 μM bR (bR/DMPC/CHAPS ratio of 1/8/330−1/3/125); (b) 1% CHAPS, 0.025% DMPC, 9.5 μM bR (1/35/1400); (c) 1% CHAPS, 0.025% DMPC, 4 μM bR (1/80/3300). The excitation was at 590 nm with 10-ns flashes of 3−6 mJ. The logarithmic time scale is from 1 to 10^7 μs.

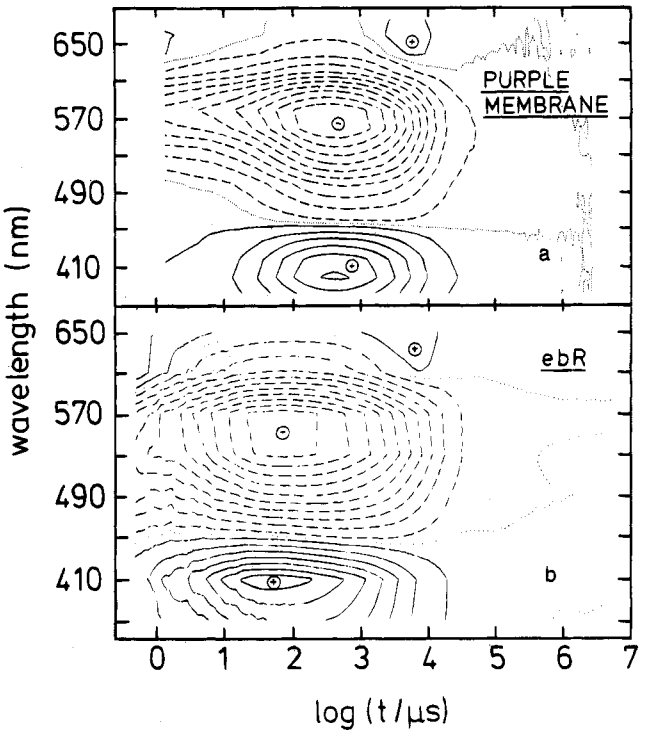

FIGURE 3: Contour plot in the (t, λ)-plane for the flash-induced absorbance changes. Lines of equal absorbance changes (positive — or negative − −) are plotted. The main maxima and minimum are labeled with + and −, respectively. The photocycle was measured in 20-nm steps from 370 to 650 nm. Excitation was as in Figure 2. (a) Photocycle of purple membrane at pH 7.3 and 22 °C. (b) Photocycle of ebR micelles in 0.1% CHAPS, 0.0025% DMPC, and 150 mM KCl, pH 7.3, at 22 °C.

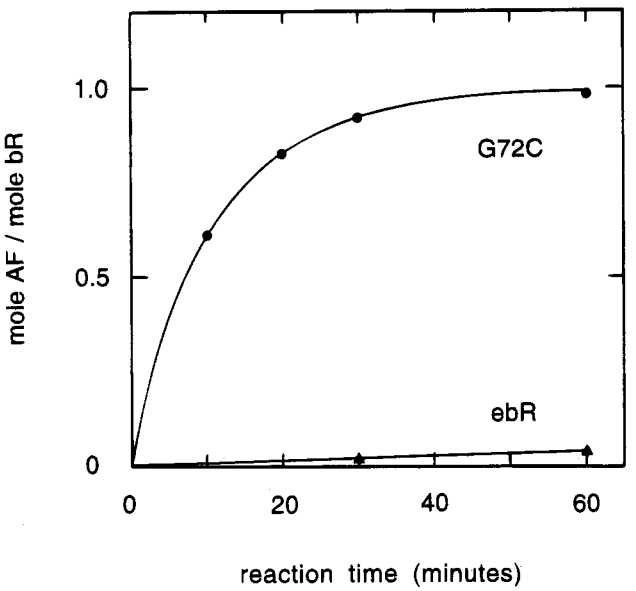

FIGURE 4: Kinetics of fluorescein incorporation into the mutant G72C and ebR. The reaction was carried out in 0.1% CHAPS, 0.0025% DMPC, 150 mM KCl, and 50 mM Tris buffer at pH 8.0 and room temperature with a 10-fold molar excess of IAF over bR. The reaction was stopped by the addition of a 100-fold molar excess of glutathione over IAF after 10-, 20-, 30-, and 60-min reaction time followed by chromatography on Sephadex G-25.

micelles. Under the above conditions, we also found a generally high stability for the reconstituted micelles over weeks. No changes in the absorbance and the photocycle kinetics were observed in the reconstituted micelles with ebR or the mutant proteins within about 2 weeks. We note from Figure 2 that the kinetics of the rise of M are virtually independent of the bR/lipid/detergent ratio. Proton release occurs in that time range.

The size of the bR micelle was calculated from the time-resolved fluorescence anisotropy of the fluorescein-labeled micelle (data not shown). An analysis based on a spherical particle led to a micelle radius of approximately 30 Å. Considering the size of DMPC and CHAPS molecules and the expected disk-like shape of the micelle which rotates slower than a sphere of equal volume, we estimated one bR molecule per micelle.

Derivatization of Cysteine Mutant bR and Characterization of Fluorescein Derivatives. Fluorescein was linked to the cysteine residues in mutant bR by reaction of its thiol group with the iodoacetamide group of IAF. To detect any unspecific reactions, we used wild-type bR micelles (ebR) as a control. An example of the rate of the reaction is shown in Figure 4 for G72C and ebR. The extent of labeling was determined spectroscopically using the alkaline absorbance band of fluorescein at 495 nm. Figure 5 shows the absorption spectrum of the mutant G72C before and after (G72C-AF) labeling with fluorescein at pH 7. The inset shows the pH dependence of the band due to bound fluorescein in steps of 0.5 unit from pH 5.5 (bottom) to pH 9.0 (top).

To verify the covalent attachment of IAF to bR, the labeled sample was subjected to SDS gel electrophoresis, and the bR band was examined for the fluorescence of fluorescein. Fluorescence was only found in the bR band of proteins containing a cysteine residue and labeled under the above conditions with IAF but not in the control run with wild type bR (ebR).

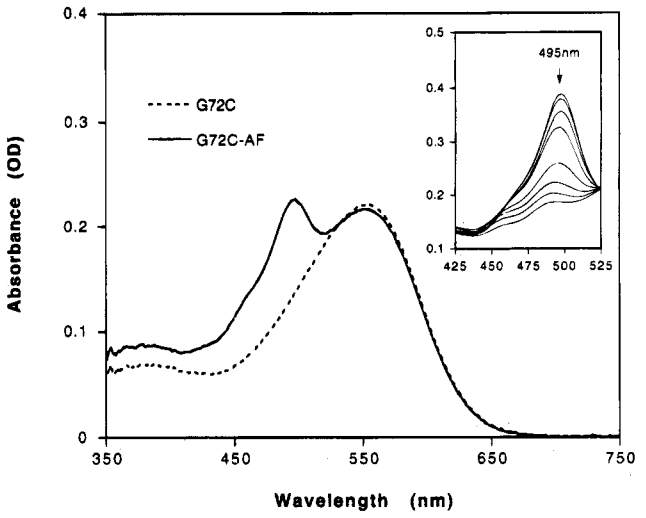

FIGURE 5: Absorption spectra of the mutant G72C before and after labeling with fluorescein (G72C-AF) at pH 7.0 in 150 mM KCl. Inset: pH dependence of the absorption spectrum of bound fluorescein (G72C-AF) from pH 9.0 (top) to pH 5.5 (bottom) in steps of 0.5 pH unit.

With a 10-fold molar excess of IAF over bR, the reaction at pH 8.0 was completed within 30 min, and about 1 mol of fluorescein was bound per mole of bR. During this time, less than 3% of fluorescein was bound to ebR (Figure 4). This reaction procedure was used for the mutant proteins with cysteine on the extracellular side in positions 72 (BC loop) and 130 (DE loop) and on the cytoplasmic side in positions 35 (AB loop), 101 (CD loop), 160 (EF loop), and 229 and 231 (carboxy terminal) (Figure 1). All mutants could be labeled in their folded active form. Generally, an incorporation of fluorescein was obtained with a stoichiometry of 0.7−1 mol of AF/mol of bR. In the position 101, only about 0.15 mol of AF/mol of bR was incorporated. The degree of labeling could be increased to about 30% when the reaction was performed in 2 M KCl. This indicates that a negative charge near 101 affects the reactivity of the sulfhydryl group in that position. Therefore, to obtain a higher incorporation of fluorescein at this position, we labeled the bacterioopsin in the denatured form resulting in the introduction of 0.7−1 mol of AF/mol of bR. Qualitatively, no differences were observed between the sample labeled before or after renaturation in respect to the absorbance, photocycle, and proton signal for this mutant.

Photocycle Kinetics and Flash-Induced Proton Concentration Changes. With fluorescein bound to the desired position in the protein, its pH-sensitive absorption band at 495 nm was used to monitor the light-induced changes in the proton concentration at these particular sites. To obtain the best signal to noise ratio, the measurements were performed near the apparent pK (pK_{app}) of fluorescein. The pK_{app} was determined for IAF after reaction with free cysteine in solution (CAF) and also when bound to the cysteine residue incorporated at the different protein sites. The pK_{app} of fluorescein in solution (as IAF or CAF) was 6.2, whereas a clearly higher pK_{app} of 7.0−7.3 (depending on labeling site) was obtained in 150 mM KCl for fluorescein bound to the bR protein surface. The increase in the pK_{app} of the bound dye was ionic strength dependent and shown to be caused by a negative surface potential (Alexiev et al., 1994a). In order to measure exclusively the light-induced absorbance changes at 495 nm as a result of proton concentration changes

Table 1: Kinetics of M Formation and Proton Release[a]

label position on the surface	M intermediate rise (μs)		H^+ release	
			DIFAF (μs)	DIFPY (μs)
ebR	0.9 (33)	9.3 (58)	69	126
extracellular				
G72C-AF	1.4 (27)	11.8 (67)	21	130
V130C-AF	1.5 (31)	11.5 (60)	22	136
cytoplasmic				
S35C-AF	1.0 (30)	9.3 (60)	61	116
V101C-AF	0.9 (33)	9.0 (57)	57	115
A160C-AF	1.1 (24)	11.3 (62)	60	115
I229C-AF	0.9 (32)	12.9 (54)	68	140
G231C-AF	1.0 (30)	11.5 (60)	61	122

[a] The M formation is measured as the absorbance increase at 410 nm in 150 mM KCl, pH 7.3, at 22 °C. The relative contributions of the two main components in the formation of M are given as percentages in parentheses following the rise times. The proton release is detected with fluorescein bound to the position indicated at 495 nm (DIFAF) and with pyranine in the aqueous bulk phase at 450 nm (DIFPY). In the case of ebR, proton release with fluorescein was measured with CAF adsorbed to the micelle.

Table 2: Kinetics of M Decay and Proton Uptake[a]

label position on the surface	M intermediate decay (ms)			H^+ uptake	
				DIFAF (ms)	DIFPY (ms)
ebR	0.4 (15)	1.8 (50)	9.8 (31)	4.3/13.1	3.8/13.8
extracellular					
G72C-AF	0.3 (12)	2.1 (51)	9.5 (31)	8.4	4.4/16.9
V130C-AF	0.4 (20)	2.3 (50)	14.3 (25)	9.1	3.5/14.0
cytoplasmic					
S35C-AF	0.3 (8)	2.0 (48)	10.6 (32)	4/18	3.7/23
V101C-AF	0.6 (28)	0.9 (30)	1.8 (30)	5.8/45	1.1/39
A160C-AF	1.1 (43)	1.9 (27)	13.5 (24)	1/13	2.1/24
I229C-AF	0.3 (73)	0.9 (17)	5.6 (4)	0.9/45	1.1/87
G231C-AF	0.7 (69)	3.2 (17)	34.9 (10)	0.8/11	1.2/28

[a] The conditions are as given in Table 1. The relative contributions of the main components in the decay of M are given as percentages in parentheses following the decay times. When two components occur in the proton uptake, the times are separated by a slash.

and not of absorbance changes cuased by transient surface potential changes (affecting the pK_{app}), the absorbance differences at 495 nm (DIFAF) between a buffered and an unbuffered labeled sample were recorded. The buffer used (10 mM MOPS) had no effect on the photocycle kinetics. The proton concentration changes in the aqueous bulk medium were measured with the negatively charged pH-indicator pyranine ($pK_a = 7.2$) at 450 nm (DIFPY, flash-induced absorbance difference with and without pyranine).

The pH dependency of the differences in the light-induced absorbance change at 495 nm was determined for the mutant V130C-AF. In the pH range of 6−8 and 150 mM KCl, the proton release kinetics remained unchanged (data not shown), whereas the amplitude of the dye signal varied with pH as expected from the pH titration data of the dye absorbance at 495 nm. The bell-shaped amplitude of the proton signal had its maximum at pH 7.3, the pK_{app} of the bound fluorescein in 150 mM KCl in the dark. Since the pK_{app} of pyranine is in the same range, all measurements were performed at pH 7.3 in 150 mM KCl.

At seven selected positions (Figure 1), the kinetics of proton release and uptake were measured with the bound fluorescein. For a meaningful comparison of the proton release data obtained for the various positions, the photocycle kinetics and the proton concentration changes detected in the bulk with pyranine must be unaltered by the introduction of the cysteine residue and also by the subsequent reaction with IAF. The time course of the photocycle at 650 and 410 nm as well as the kinetics of proton release and uptake, detected by fluorescein bound to the protein surface and by pyranine in the aqueous bulk phase, were measured. The kinetic data for ebR and the mutants are summarized in Tables 1 and 2. The kinetics of the M-intermediate are shown in Figure 6 for the labeled mutants on the cytoplasmic side and in Figure 7 for the mutants on the extracellular side. The absorbance traces (M-intermediate and proton concentration changes measured with fluorescein, DIFAF, and pyranine, DIFPY) for ebR and three selected mutants (S35C-AF, G72C-AF, G231C-AF) are presented in Figure 8.

(A) Proton Release and Uptake in ebR. The proton release and uptake were measured in ebR with the pH-indicator pyranine in the aqueous bulk phase and also with fluorescein

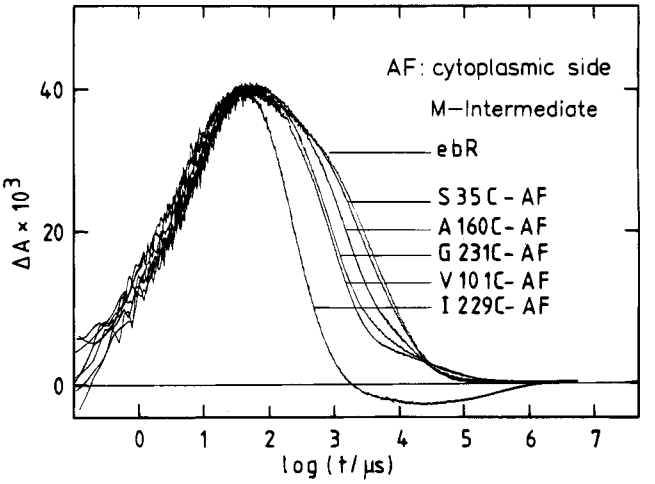

FIGURE 6: Flash-induced absorbance changes at 410 nm for bR mutants with fluorescein attached to cysteine residues on the cytoplasmic side as indicated and ebR as control. Sample conditions as in Figure 2a.

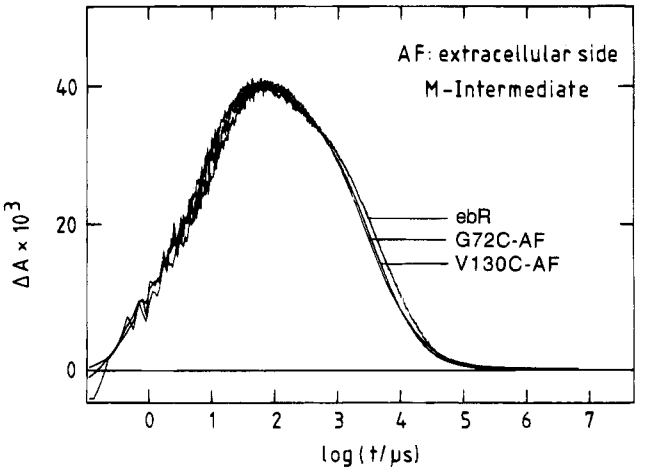

FIGURE 7: Flash-induced absorbance changes at 410 nm for ebR and the two mutants G72C and V130C with fluorescein attached to the positions 72 and 130, respectively, on the extracellular side. Sample conditions as in Figure 2a.

added as CAF in solution (CAF is IAF bound to free cysteine) (Figure 8). The proton release time measured with CAF is much faster ($\tau \approx 60-70$ μs) than that detected with pyranine ($\tau \approx 120-130$ μs) in the bulk phase. Since CAF is more hydrophobic than the negatively charged pyranine, it is probably adsorbed to the micelle surface leading to a

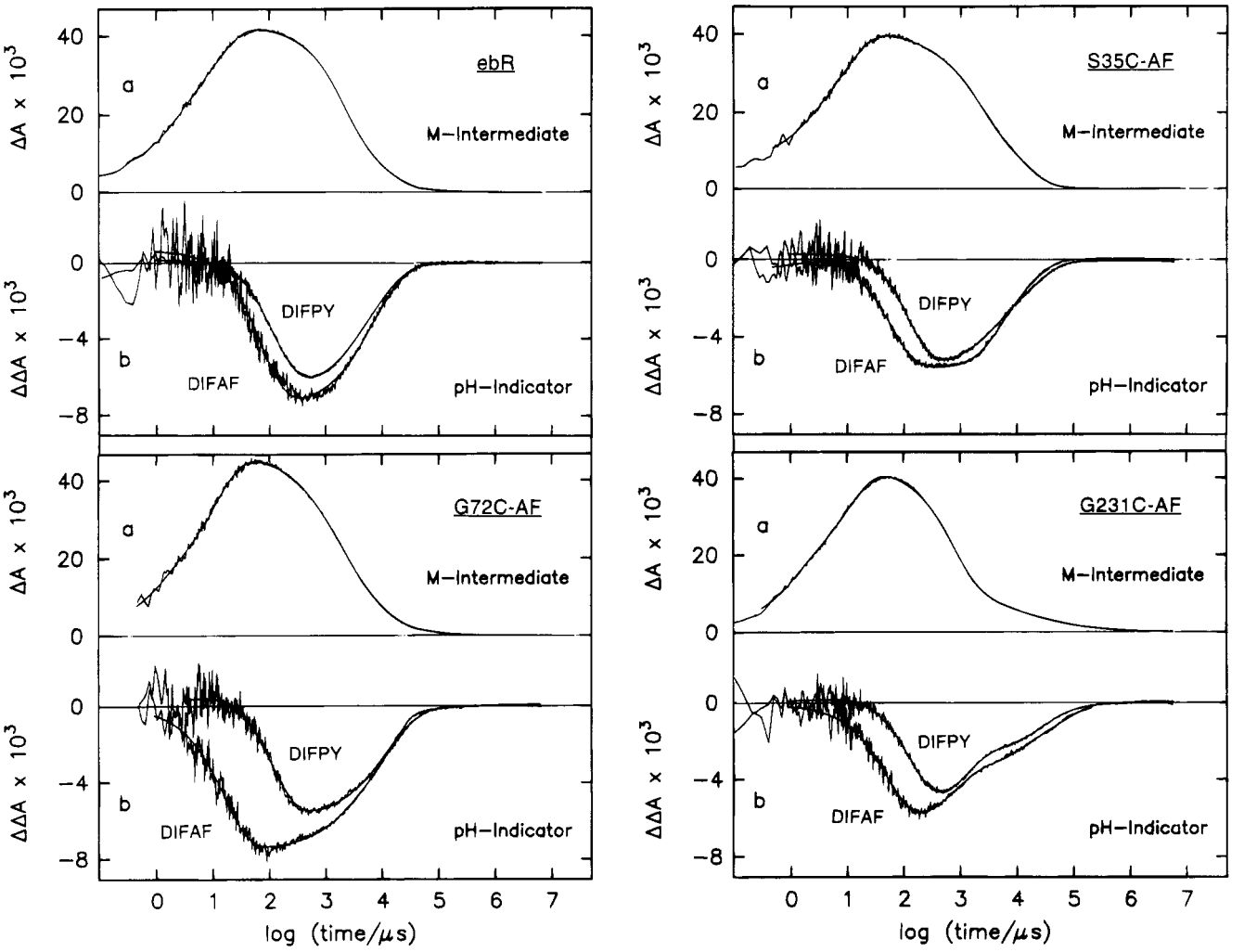

FIGURE 8: Comparison of the rise and decay of the M intermediate at 410 nm (a) with the kinetics of the proton release and uptake (b) for wild-type and selected mutants. In b, the proton signal as detected by bound fluorescein (CAF in the case of ebR) at 495 nm is the absorbance difference between unbuffered and buffered (10 mM MOPS) samples (DIFAF). The proton signal in the bulk as sensed by pyranine at 450 nm is the absorption difference between samples with and without pyranine (DIFPY). A negative $\Delta\Delta A$ indicates the release of protons. The solid lines represent multiexponential fits. The samples were in 0.1% CHAPS, 0.0025% DMPC, and 150 mM KCl, pH 7.3, at 22 °C. The excitation was at 590 nm with 10-ns flashes of 3−6 mJ. The logarithmic time scale is from 1 to 10^7 μs.

faster detection of proton release.

(B) Proton Release and Uptake Detected with Fluorescein Attached to Loop Regions on Extracellular Side. When glycine in position 72 and valine in 130 were replaced by cysteine, the absorbance and the photocycle kinetics of the mutants were virtually unchanged compared to wild-type bR. The attachment of fluorescein to these positions affected neither of the above parameters (Figures 7 and 8). The light-induced absorbance changes at 410 nm for the M-intermediate and the proton signal measured with the pH-indicator dyes fluorescein at 495 nm (DIFAF) and pyranine at 450 nm (DIFPY) are shown in Figure 8.

The proton release time of about 20 μs detected with the bound fluorescein in positions 72 and 130 is six times faster than the one measured with pyranine ($\tau \approx 130$ μs). The proton uptake kinetics detected with pyranine and bound AF are approximately identical and follow the M decay. The proton uptake kinetics measured with fluorescein contains an additional minor component (10−15%) with a time of about 120 μs. The proton release times obtained with pyranine in the bulk phase are similar in ebR and the cysteine mutants as expected from their identical photocycle kinetics.

(C) Proton Release and Uptake Detected with Fluorescein Bound to Loops on Cytoplasmic Side. Fluorescein was bound to position 35 in the AB loop, 101 in the CD loop, 160 in the EF loop, and 229 and 231 in the C-terminal tail. These mutants with cysteine on the cytoplasmic side showed both before and after labeling with IAF the same absorption maxima as ebR. The photocycle kinetics for S35C and A160C were similar to ebR, whereas for V101C, I229C, and G231C, changes in the later part of the photocycle (M decay) were detected. The subsequent labeling did not significantly change the photocycle. Figure 6 shows the rise and decay of the M-intermediate for wild-type and cytoplasmic mutants after labeling. The rise time of M is within a very narrow range identical for all mutants and wild type. For the kinetics of the proton release, the formation of M is the relevant process. The detection times of the released proton with fluorescein in all positions on the cytoplasmic surface are quite similar ($\tau = 61 \pm 4$ μs, see Table 1) and approximately three times slower than in the loop positions on the extracellular side. They are clearly faster than the release times detected with pyranine in the bulk phase ($\tau \approx 120$ μs). The changed kinetics in the M decay had no effect on

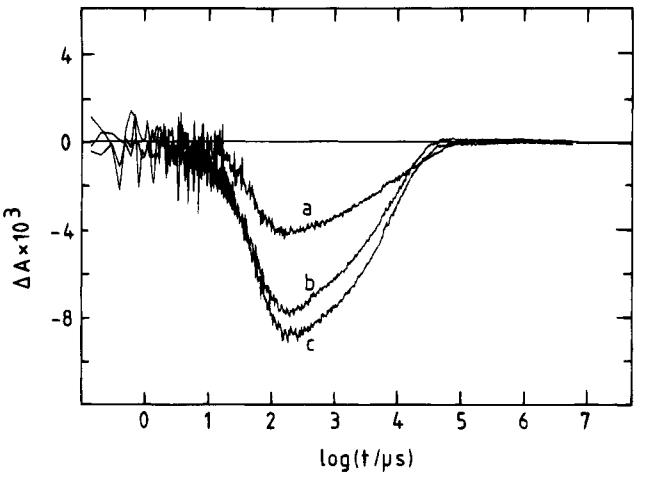

FIGURE 9: Effect of the phospholipid headgroups in mixed micelles on the amplitude of the flash-induced proton signal measured with fluorescein attached to position 35 on the cytoplasmic surface. The difference of the flash-induced absorbance changes is shown at 495 nm of S35C-AF between an unbuffered and buffered (10 mM MOPS) sample in 150 mM KCl, pH 7.3, at 22 °C and the following: (a) 0.1% CHAPS, 0.002% DMPA; (b) 0.1% CHAPS; (c) 0.1% CHAPS, 0.05% DMPC.

the proton release times, whereas clear differences were observed in the proton uptake kinetics which occur roughly in parallel to the M decay kinetics (Figure 8; Tables 1 and 2).

Dependence of Proton Signal on Micelle Composition. The fact that the proton released on the extracellular side of bR is detected faster on the cytoplasmic side than in the aqueous bulk phase suggests that the protons may be retained at the surface by fixed buffer groups (acidic and basic groups) of bR and the micelle and that they migrate along the micellar surface to the opposite side. To test this possible interpretation, the proton mobility along the micellar surface was varied by adding phospholipids with headgroups of different pK_a's to the CHAPS/bR micelles. Similar experiments have been performed with neutral detergent micelles in which the source of the transient protons was in the bulk medium (Nachliel & Gutman, 1988). The idea behind these experiments is that the dwell time of protons on the lipid and detergent headgroups (the inverse of the dissociation rate constant) increases rapidly with their pK (Gutman & Nachliel, 1990). We therefore added DMPC (0.05%) with a pK of 2.2 or DMPA (0.002%) with a pK of 8.0 to the bR/CHAPS micelles. The pK of the sulfate group of CHAPS at the micelle/water interface is around 4. The amount of DMPC and DMPA added were chosen in such a way that the three micelle preparations of Figure 9 had approximately the same buffer capacity (as measured by the ratio of the change in fluorescein absorbance and the change in bulk proton concentration). DMPC with a dwell time of only 9 ns is expected to enhance the proton mobility along the surface, whereas DMPA with a dwell time of around 10 ms will reduce it. The effect of these lipid additions on the proton release kinetics detected with fluorescein at position 35 on the cytoplasmic side is shown in Figure 10. Addition of DMPC (trace c) or DMPA (trace a) led to an increase and decrease, respectively, in the amplitude of the proton signal as compared to the control bR/CHAPS micelles (trace b). With the label on the extracellular side at position 130 (the proton release side), the same lipid additions had no effect (data not shown).

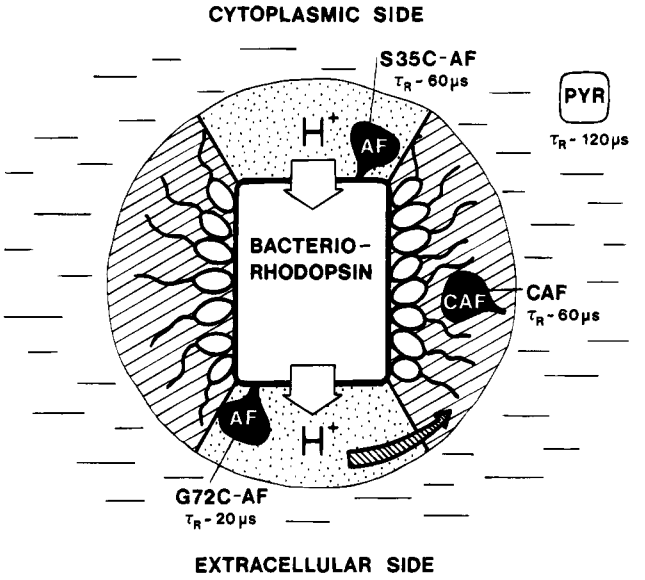

FIGURE 10: Cartoon of the bR micelle with the proton release times as detected at the various positions on the surface and in the bulk as indicated. The CHAPS molecules are drawn schematically according to their chemical structure with a hydrophobic head and a hydrophilic tail. The boundary layer protein-bulk and detergent/lipid-bulk are marked by stippling and hatching, respectively.

DISCUSSION

Bacteriorhodopsin monomers have been shown to be active in light-induced proton pumping, and furthermore, in natural isolated Halobacteria, bR is often not aggregated into purple membrane patches (Bivin & Stoeckenius, 1986; Otomo et al., 1992). This indicates that the aggregated state of bR in the purple membrane is not necessary for its function, and therefore, bacteriorhodopsin in micelles offer a useful system for the study of the kinetics of light-induced proton release and uptake during the bR photocycle. The conditions now described for the bR−micelle system lead to highly reproducible photocycle kinetics that are quite similar to those of the native purple membrane. The photocycle kinetics do not depend on the concentrations of the lipid, detergent, and protein components but on their molar ratios, which have been specified. Under these conditions (0.1% CHAPS and 0.0025% DMPC in 150 mM KCl), small variations in the protein concentration (4−10 μM) had virtually no effect on the photocycle kinetics. At 0.1% CHAPS, we are below the critical micellization concentration (cmc for CHAPS in 150 mM KCl is 0.3%). Furthermore, changing the CHAPS concentration from 0.1% to 0% caused only minor effects on the photocycle kinetics, and moreover, the bR molecules did not aggregate. This indicates a strong binding of the CHAPS molecules to the hydrophobic domains of the protein, the areas that are presumably in contact with the lipids in the membrane (Figure 10).

In the micelle system as well as for purple membranes, the previously reported proton release times detected with the pH-indicator pyranine in the aqueous bulk phase are about 10-fold longer than the rise time of the main component of M formation (10 μs/120 μs and 50 μs/500 μs for M rise/proton release signals in micelles and purple membranes, respectively). The proton release kinetics in purple membrane as detected by pyranine is accelerated in the presence of low buffer concentrations (Drachev et al., 1984; Grzesiek

& Dencher, 1986), indicating a faster appearance of the proton on the protein surface than that sensed by the indicator in the bulk. With free fluorescein (CAF) added to the micellar suspension, we detected a faster proton release kinetics than with the negatively charged pyranine (69 μs compared to 126 μs). We attribute this accelerated detection of the proton to fluorescein being adsorbed to the micelles because of its somewhat hydrophobic character. This interpretation is supported by the observation that a Sephadex G-25 column of larger size than the theoretical one was required to remove fluorescein (CAF or IAF) from ebR micelles. With purple membrane, the same proton release times were observed with fluorescein and pyranine, presumably because fluorescein did not adsorb to the purple membrane patches (data not shown). Heberle et al. (1992) bound fluorescein covalently to the ϵ-amino group of lysine(s) on the surface of the purple membrane and observed a release time of $\approx$70 μs compared to about 500 μs in the aqueous bulk phase.

In the present work, we developed a versatile method for covalently attaching a pH-sensitive indicator dye (fluorescein) to different sites on the extracellular and cytoplasmic surface, the proton release and uptake side, respectively. We used bR mutants with single cysteine residues in various positions on the protein surface and bound fluorescein covalently to their sulfhydryl groups by specific reaction with IAF. The labeling with IAF affected neither the absorbance spectrum nor the photocycle kinetics. All of the cysteine mutants used show wild-type-like kinetics in the earlier part of the photocycle, while the decay from M to bR was only changed in some mutants with cysteine on the cytoplasmic, the proton uptake side.

The later part of the photocycle (M to bR) during which a proton is taken up from the cytoplasmic side is extremely sensitive to amino acid replacements on that surface (see Figure 6), suggesting a role of the surface structure in the proton uptake. Changes in the kinetics in this part of the photocycle are also observed in partially delipidated purple membrane and when lipids were exchanged for detergent molecules (Fukuda et al., 1990) and may be interpreted as the result of structural alterations. The largest changes in the photocycle kinetics were observed in mutant proteins with amino acid replacements near helix G. Structural changes in this helix in the bR to M transition were observed by neutron diffraction (Dencher et al., 1989), and these were localized on the cytoplasmic side of this helix (Subramaniam et al., 1993). Since all the observed changes in the photocycle of the various mutants occur after the proton is released, these mutants can be used to investigate and compare the proton release times in the various positions. A comparison among the uptake times is clearly not meaningful.

Using the probes attached to either side of the bR surface to monitor proton release, we found that the release kinetics detected on the extracellular, the proton release side (positions 72 and 130), were approximately three times faster than those measured on the cytoplasmic, the proton uptake side (positions 35, 101, 160, 229, and 231) (22 $\pm$ 4 μs versus 61 $\pm$ 4 μs). Most significant is the finding that the release kinetics, observed on either side, were clearly faster than those detected with pyranine in the aqueous bulk phase. The proton release times measured with pyranine were similar in all samples and indistinguishable from wild type as expected, since they all show similar M-rise kinetics. The faster proton release times detected with AF on both protein surfaces suggest that the released proton moves faster along the micellar surface than into the aqueous bulk phase. The proton is apparently retarded at the surface by protonatable groups. Moreover, the protonation rate of pyranine by collisions with the surface is expected to be low due to the high negative charge of the dye and the negative charge of the protein surface (Alexiev et al., 1994a). The idea that the proton is retained at the surface is supported by the observation that the release times in the microsecond range detected on the extracellular and cytoplasmic side of bR differ substantially (by 30−40 μs) in spite of the fact that the micelles tumble on the nanosecond time scale. The rotational correlation time of the micelles, as determined from the time-resolved fluorescence depolarization of the bound AF, was less than 50 ns (data not shown). If the protons were not trapped at the surface, one would expect that on the microsecond time scale the rapid tumbling would lead to the observation of equal release times with labels on the two sides.

If the protons do move along the micellar surface, lipid and detergent headgroups would be expected to play a major role, and therefore, a change in their charge and pK_a's should affect the mobility of the proton. Previous investigations (Gutman & Nachliel, 1985; Nachliel & Gutman, 1988) indeed showed that the proton movement along the surface of lipid vesicles and micelles was affected by the pK_a of the surface groups. A group with a higher pK_a retains a proton much longer than a group with a lower pK_a (for phosphatidylserine with a pK_a of 4.6, the dwell time $\tau_D \approx 4$ μs; for phosphatidylcholine with a pK_a of 2.2, $\tau_D \approx 10$ ns). As a consequence, protons diffuse over longer distances in the presence of low pK_a headgroups, allowing many hopping steps, and over shorter distances with higher pK_a headgroups, delaying the proton and reducing its mobility. If in the present experiments proton migration along the micellar surface is the major pathway for the protonation of the dye molecule on the cytoplasmatic side, one would expect that the addition of lipids with headgroups of a lower pK_a than the SO_3^- group of CHAPS (p$K \approx 4$) will lead to an increase in the amplitude of the protonated dye signal, whereas addition of lipids with higher pK_a headgroups will result in a reduction. With the dye on the extracellular side, where the proton is released, no proton migration along the micellar surface is necessary to reach the dye molecule; therefore, no effect by the lipid headgroups should be expected. The cartoon of a bR micelle shown in Figure 10 summarizes the experimentally observed proton release times and the interpretations presented above. Experimental support for the model was obtained as shown in Figure 9. The lipid composition in the micelles was changed by adding either DMPC (pK_a of 2.2) or DMPA (pK_a of 8.0, $\tau_D \approx 10$ ms). With the dye on the cytoplasmic side (S35C-AF), a decrease in the fluorescein amplitude was observed upon the addition of DMPA, and an increase in the amplitude was observed with DMPC (Figure 9). The signal amplitude for fluorescein on the extracellular side was not affected by the addition of either DMPA or DMPC. These data support the idea that the proton released on the extracellular side is moving along the micellar surface faster than it transfers to the aqueous bulk phase and, therefore, is sensed faster by a surface-bound dye on the cytoplasmic side than by pyranine in the bulk. Our findings of efficient proton migration along the surface

of bR micelles and their delayed appearance in the bulk support the concepts of localized proton coupling along the membrane surface. In our current work, we have confirmed and extended these observations with purple membrane (Alexiev et al., in press).

ACKNOWLEDGMENT

We thank Sabine Flitsch for the G72C mutant, Ellen van den Berg de Brabander for the I229C and G231C mutants, and Susanne J. Marti for technical assistance in the preparation of mutants.

REFERENCES

Alexiev, U., Marti, T., Heyn, M. P., Khorana, H. G., & Scherrer, P. (1994a) *Biochemistry 33*, 298−306.

Alexiev, U., Marti, T., Heyn, M. P., Khorana, H. G., & Scherrer, P. (1994b) *Biochemistry 33*, 13693−13699.

Bivin, D. B., & Stoeckenius, W. (1986) *J. Gen. Microbiol. 132*, 2167−2177.

Dencher, N. A., Dresselhaus, D., Zaccai, G., & Büldt, G. (1989) *Proc. Natl. Acad. Sci. U.S.A. 86*, 7876−7879.

Drachev, L. A., Kaulen, A. D., & Skulachev, V. P. (1984) *FEBS Lett. 178*, 331−335.

Flitsch, S. L., & Khorana, H. G. (1989) *Biochemistry 28*, 7800−7805.

Fothergill, J. E. (1964) in *Fluorescent Protein Tracing* (Nairn, R. C., Ed.) pp 34−59, E&S Livingstone Ltd., Edinburgh and London.

Fukuda, K., Ikegami, A., Nasuda-Kouyama, A., & Kouyama, T. (1990) *Biochemistry 29*, 1997−2002.

Grzesiek, S., & Dencher, N. A. (1986) *FEBS Lett. 208*, 337−342.

Gutman, M., & Nachliel, E. (1985) *Biochemistry 24*, 2941−2946.

Gutman, M., & Nachliel, E. (1990) *Biochim. Biophys. Acta 1015*, 391−414.

Heberle, J., & Dencher, N. A. (1990) *FEBS Lett. 277*, 277−280.

Heberle, J., & Dencher, N. A. (1992) *Proc. Natl. Acad. Sci. U.S.A. 89*, 5996−6000.

Kano, K., & Fendler, J. H. (1978) *Biochim. Biophys. Acta 509*, 289−299.

Lanyi, J. K. (1992) *J. Bioenerg. Biomembr. 24*, 169−179.

Lewis, A., Spoonhower, J., Bogomolni, R. A., Lozier, R. H., & Stoeckenius, W. (1974) *Proc. Natl. Acad. Sci. U.S.A. 71*, 4462−4466.

Liao, M.-J., London, E., & Khorana, H. G. (1983) *J. Biol. Chem. 258*, 9949−9955.

London, E., & Khorana, H. G. (1982) *J. Biol. Chem. 257*, 7003−7011.

Lozier, R. H., Bogomolni, R. A., & Stoeckenius, W. (1975) *Biophys. J. 15*, 955−962.

Lozier, R. H., Niederberger, W., Bogomolni, R. A., Hwang, S. B., & Stoeckenius, W. (1976) *Biochim. Biophys. Acta 440*, 545−556.

Marti, T., Rösselet, S. J., Otto, H., Heyn, M. P., & Khorana, H. G. (1991) *J. Biol. Chem. 266*, 18674−18683.

Milder, S. J., Thorgeirsson, T. E., Miercke, L. J. W., Stroud, R. M., & Kliger, D. S. (1991) *Biochemistry 30*, 1751−1761.

Nachliel, E., & Gutman, M. (1988) *J. Am. Chem. Soc. 110*, 2629−2635.

Oesterhelt, D., & Stoeckenius, W. (1971) *Nature (London), New Biol. 233*, 149−152.

Oesterhelt, D., Tittor, J., & Bamberg, E. (1992) *J. Bioenerg. Biomembr. 24*, 181−191.

Otomo, Y., Tomioka, H., & Sasabe, H. (1992) *J. Gen. Microbiol. 138*, 1027−1037.

Otto, H., Marti, T., Holz, M., Mogi, T., Lindau, M., Khorana, H. G., & Heyn, M. P. (1989) *Proc. Natl. Acad. Sci. U.S.A. 86*, 9228−9232.

Rothschild, K. J. (1992) *J. Bioenerg. Biomembr. 24*, 147−167.

Scherrer, P., Packer, L., & Seltzer, S. (1981) *Arch. Biochem. Biophys. 212*, 589−601.

Scherrer, P., Alexiev, U., Otto, H., Heyn, M. P., Marti, T., & Khorana, H. G. (1992) in *Structures and Functions of Retinal Proteins* (Rigaud, J. L., Ed.) Vol. 221, pp 205−211, Colloque INSERM, John Libbey Eurotext Ltd., Montrouge, France.

Stoeckenius, W., & Bogomolni, R. A. (1982) *Annu. Rev. Biochem. 52*, 587−615.

Subramaniam, S., Gerstein, M., Oesterhelt, D., & Henderson, R. (1993) *EMBO J. 12*, 1−8.

Váró, G., & Lanyi, J. K. (1990) *Biochemistry 29*, 6850−6865.